Journal of Physics: Conference Series **3010** (2025) 012025 doi:10.1088/1742-6596/3010/1/012025

Progress in Design of Permanent Magnet Dipole-Quadrupoles with Longitudinal Gradient for the PETRA IV Storage Ring

M. Gehlot*[1], T. Ramm[1], M. Tischer[1], P. Vagin[1], J. Chavanne[2]

[1] DESY, Hamburg, Germany
[2] ESRF, Grenoble, France

*E-mail: mona.gehlot@desy.de

Abstract. PETRA IV is an upgrade project planned to replace the Synchrotron light source PETRA III. The main objective is to reduce the horizontal emittance to 20 pmrad. This nominal emittance will be achieved by a hybrid six bend achromat lattice(H6BA). To fulfill the requirement of this lattice, three different types of permanent dipole magnets will be used which include a combined-function dipole-quadrupole magnet with both longitudinal and transverse gradient (DLQ). The use of permanent magnet material for the combined-function dipole-quadrupole magnets is particularly useful for achieving a compact design, but also for reducing power consumption during operation. This paper presents the overall progress in this DLQ development, the expected magnetic field characteristics obtained from 3D Radia simulations, and advanced design details like the cross-talk with neighboring quadrupole magnets. The status of the present prototype activities is also discussed.

1. Introduction

The PETRA III storage ring is a light source operating at 6 GeV and will be replaced by PETRA IV [1,2]. The storage ring will be completely rebuilt with a hybrid six-bend lattice (H6BA) in order to achieve the low emittance by using longitudinal gradient dipoles. For the PETRA IV storage ring, several permanent magnet combined-function longitudinal gradient dipole-quadrupoles (DLQ) will be built. Following the successful implementation of permanent magnet dipoles at the ESRF for the previous EBS upgrade [3,4], many other synchrotron facilities are using permanent magnet dipoles [5-6] for their upgrades, such as SLS2.0, Diamond-II, and SOLEIL II. The PETRA IV DLQ comprises a transversely tapered field in order to produce an additional quadrupole component. The use of permanent magnet combined-function magnets offers several key advantages. They enable precise control of particle beam trajectories while simultaneously providing the necessary focusing and bending properties. This results in a more compact and efficient accelerator layout. Additionally, the elimination of power supplies and cooling systems associated with conventional electromagnets reduces the overall complexity and operational footprint of the accelerator.

The Radia software [7] is used for magnetic simulations to design the DLQ's pole shape and yoke. Mechanical design follows the magnetic design. The fabrication of a first DLQ prototype is underway. Three different types of permanent magnet dipoles will be used in the H6BA cell as illustrated in Figure 1. Out of three dipole magnets, one has both transverse and longitudinal gradients which is DLQ1. As detailed in our previous article [8], the lattice values and design features of the DLQs include a C-shaped yoke with a compact cross section of about 120×200 mm^2 (w × h). Figure 2 describes the cross-section of the three different DLQs. The yoke and poles are made of soft iron. The magnetic material used for the DLQ is SmCo. This paper describes the 3D simulation results for the field quality of two types of combined-function magnets, one with longitudinal gradient (DLQ1) and one without (DLQ2).

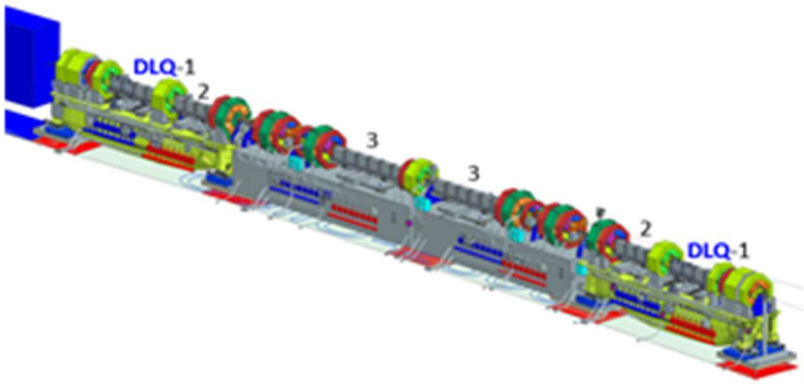

Figure 1. PETRA IV storage ring H6BA lattice showing DLQ-1,2,3 magnets.

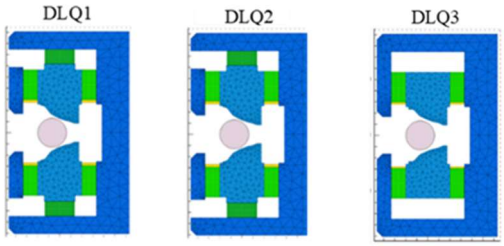

Figure 2. Cross section of combined-function dipoles in the magnetic model; thermal shims (yellow) are placed on top of the permanent magnets (green).

2. 3D design details of combined-function dipoles

2.1 Design details of DLQ1

The magnet design is developed by means of Radia in two steps, 2D and 3D simulations. The overall design of poles, yoke and PMs is done by 2D simulation studies, i.e. excluding all end effects. Once the required field and gradient were obtained from 2D calculations for a single module, 3D simulations were performed to study the end field effects of a single module and finally the crosstalk between the modules. Thin endpole pieces had been attached at both ends of all modules and slightly reshaped from the nominal pole contour so that they compensate the end effects. Different geometries of endpoles are used at the ends and between the modules in order to account for the different effects at both interfaces. Small dips in the field and gradient arise at

the module interfaces which originate from a small 4mm air gap in between modules included for mechanical reasons. The required field quality is then obtained using a pole shape optimization algorithm which flattens the remaining field errors. These are defined as the quadratic sum of all field harmonics $\sqrt{\sum_{i=1}^{N} B_i^2}$ with a maximum value of 5×10^{-4}. For faster optimization, the field properties were for now evaluated along a straight trajectory through the DLQ. The integrated field and gradient value for DLQ1 are -0.314 Tm and -12.3 T, respectively. A comparison of the lattice magnetic field and gradient with the simulated are shown in Figure 3. Longitudinal progression of higher-order components is calculated within a radius of 11 mm to optimize the basic field quality. Figure 4 shows the sextupole and octupole components along the longitudinal position with an integrated value of -0.562 T/m and 18.89 T/m^2, respectively.

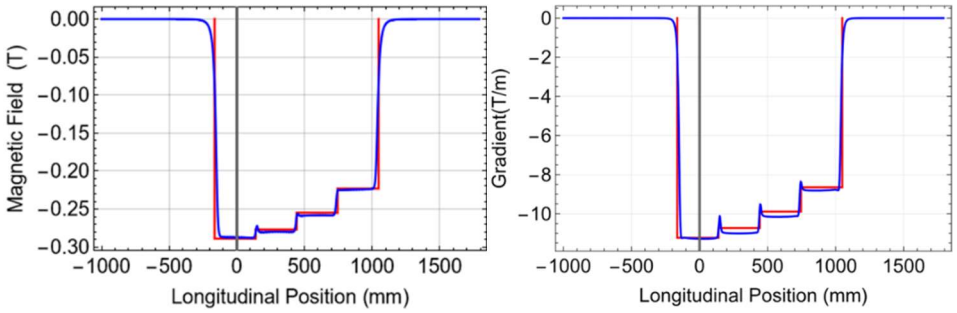

Figure 3. Longitudinal dependence of field and gradient of DLQ1 as simulated (blue) in comparison to lattice values (red).

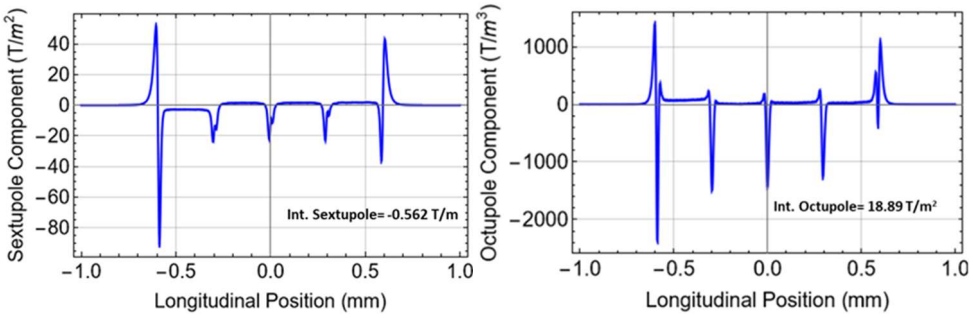

Figure 4. Longitudinal variation of sextupole and octupole components within a radius of 11mm.

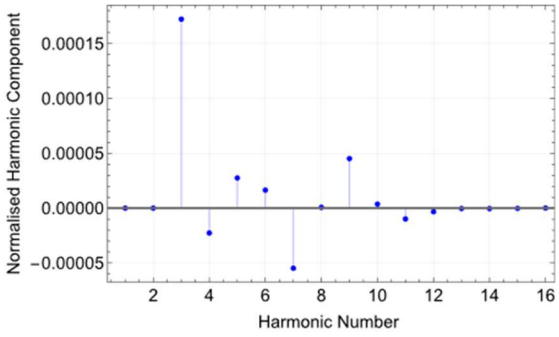

Figure 5. Higher harmonics (normalized to integrated dipole) result in 1.9×10^{-4} for the quadratic sum of all components.

This information is relevant for assessing the higher-order field effects in the magnet design, which can impact beam dynamics and stability in particle accelerators. Together, these figures provide valuable insights into the operational parameters and quality of the magnetic fields produced by the DLQ1 magnet. A tuning margin with iron shims must be included in the magnetic design for precise adjustment of field strength, gradient and even for correction of sextupole errors. The analysis of higher field harmonics, which are normalized to the integrated dipole component, is seen in Figure 5. The quadratic sum of field harmonics amounts to 1.9×10^{-4}, well within the required specifications. In a final design step, four modules are arranged to a full DLQ1 along the curved trajectory, i.e. at a small angle and offset from each other, and all modules are locally compensated for crosstalk with adjacent quadrupoles to achieve the nominal values for integrated field and integrated gradient. The crosstalk studies are described in more detail in the following section.

2.2 Design details of DLQ2

The DLQ2 dipole is designed as well with a transverse gradient, but consists of four identical modules. It succeeded to match the specified values for field amplitude and gradient by means of the same cross-section and pole shape as DLQ1 which is regarded as a significant simplification of the mechanical design. The key distinction is that DLQ2 operates with a lower magnetic field, resulting in a reduced filling factor compared to DLQ1. For reference, the integrated field and gradient values for DLQ2 are -0.204 Tm and -8.4 T, respectively. The field-to-gradient ratio for DLQ2 is noted to be 24.5 mm. Figure 6 presents a comparison between the lattice values and simulation results for the field and gradient of DLQ2.

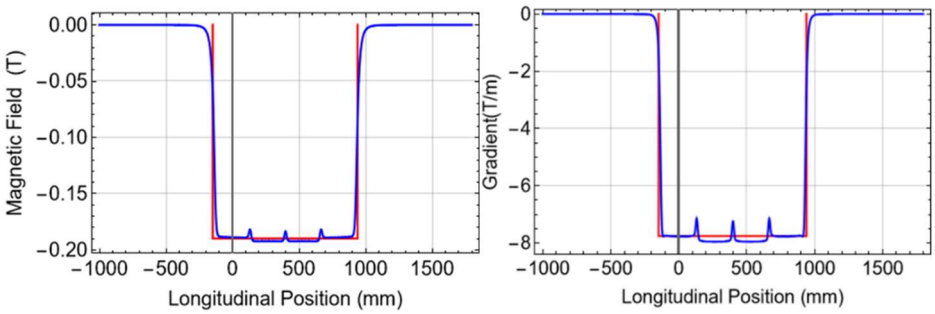

Figure 6. Longitudinal field and gradient dependence of DLQ2 as simulated (blue) in comparison to lattice values (red).

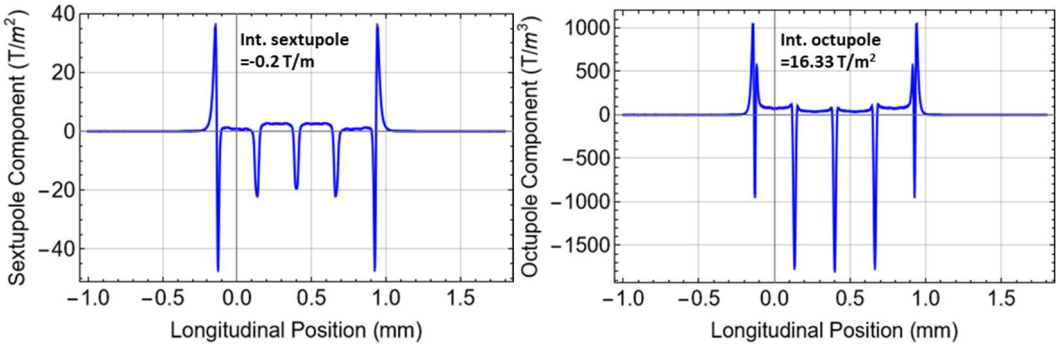

Figure 7. Longitudinal variation of sextupole and octupole component of DLQ2 within a radius of 11mm.

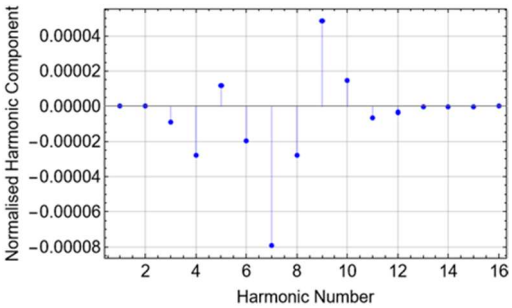

Figure 8. Higher harmonics (normalized to integrated dipole) amount to 1.05×10^{-4} for the quadratic sum of all components.

In Figure 7, the longitudinal variation of sextupole and octupole components is depicted, resulting in values of 0.2 T/m for the integrated sextupole and 16.33 T/m^2 for the integrated octupole. Figure 8 shows the normalized higher harmonic components which add up to a quadratic sum of 1.05×10^{-4}, well within the required specifications.

3. Crosstalk studies of DLQ1 with quadrupoles

A significant amount of magnetic cross-talk has been observed between the DLQs and neighbouring quadrupole magnets. The DLQ1 is surrounded by two high-gradient quadrupoles, PQC and PQD with a defocusing and focusing gradient of -86 T/m and +97 T/m respectively (Figure 9). The distance between PQC and DLQ1 is only 63 mm while it is 105 mm between DLQ1 and PQD. For the high-field module M4 of DLQ1, a significant reduction in integrated field and gradient was found, 0.5% and 1.44% respectively. At the opposite end at the low-field module M1 close to PQD, an increase in integrated field and gradient by 0.33% and 0.75% was found, respectively. Figure 10 shows the longitudinal variation of magnetic field and gradient before and under the influence of the two quadrupoles together with the crosstalk as the corresponding differences. It can also be seen that the crosstalk effects propagate across all four modules.

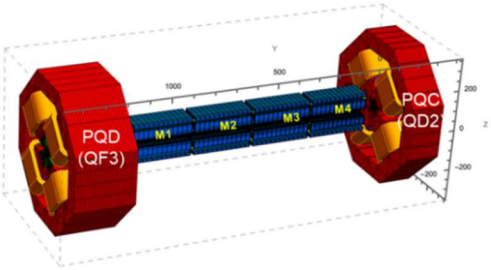

Figure 9. Full 3D magnetic model of DLQ1(in blue) surrounded with quadrupoles PQC and PQD (in red).

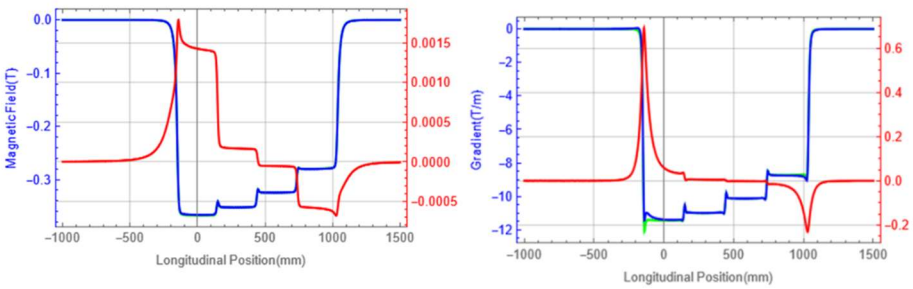

Figure 10. Simulation of field (left) and gradient (right) of the full DLQ1 alone (green curve) and influenced by the quadrupoles (blue curve); the difference is plotted on the opposite axis (red curve).

The simulation was carried out for the full DLQ1 and the overall effect on the full DLQ1 in terms of integrated field and gradient is of the order of +0.085% and +0.24%, respectively. To mitigate the crosstalk effects locally, an individual correction has been made in all modules by a slight adjustment of the permanent magnet filling factor. In turn, the DLQ1 also impacts the neighboured quadrupoles and induces small dipole fields adding up to +0.3 Tmm in PQC and -0.15 Tmm in PQD. Such small values could easily be corrected by a tiny quadrupole displacement in the order of a few 10 μm. Similar crosstalk studies are ongoing for DLQ2.

4. Prototype and measurement activities

The magnetic layout has been transferred to a mechanical design of all modules of DLQ1 together with an adjustable support base. Three manufacturers are currently constructing prototype modules, and we anticipate initial deliveries soon, as most small parts are already in place. For magnetic measurements, we are utilizing a stretched wire bench for the DLQs. We have simulated and analyzed potential positioning errors which create distinct field error signatures across various measured quantities like 1st and 2nd field integrals of both field components. These will be used for alignment during characterization process. The differences between a field analysis along a straight line and along the curved trajectory have been investigated in depth; notable differences are found in the absolute values of field integral (5×10^{-3} Tmm) and integrated gradient (7.3×10^{-4} T) due to the longer path length of the curved trajectory (~60 μm). A Hall probe bench which is available in the prototype phase will be used to address such special characterization topics of the DLQ. It will also allow for mapping fringe fields at the module's outer ends and the inner interfaces.

5. Conclusion

Three different permanent magnet-based combined-function dipole magnets are presently developed for PETRA. The required lattice parameters and field quality are successfully achieved even for the design complexity of DLQ1 with a longitudinal gradient. The mechanical design of DLQ1 is accomplished. Only minor adaptions to this are needed to derive the design for DLQ2. Manufacturing of DLQ1 prototype modules is nearly completed. Tooling for module assembly is available, preparations for magnetic measurements are progressing. The cross-talk between DLQ1 and its neighbouring quadrupoles has a measurable impact on field and gradient of DLQ1. Although the overall effect is relatively small, a local correction approach will help in mitigating these effects, ensuring that the properties of the DLQ1 remain well within lattice specification.

References

[1] R. Bartolini et al., "Status of PETRA IV Machine Project", in Proc. IPAC2022, Bangkok, Thailand, doi:10.18429/JACoW-IPAC2022-TUPOMS029.
[2] I. Agapov et al., "Magnet Design for PETRA IV Storage Ring", in Proc. IPAC2022, Bangkok, Thailand, doi:10.18429/JACoW-IPAC2022-THPOTK002
[3] G. Le Bec *et al*., "Magnets for the ESRF Diffraction-Limited Light Source Project," in *IEEE Transactions on Applied Superconductivity*, vol. 26, no. 4, pp. 1-8, June 2016.
[4] C. Benabderrahmane, et al., "Status of the ESRF-EBS-Magnets", in *Proc. IPAC'18*, Vancouver, Canada, 2018.
[5] B.J.A. Shepherd et al., "Permanent magnets for accelerators", in Proc. IPA2020, Caen, France, doi:10.18429/JACoW-IPAC2020-MOVIRO05.
[6] J. Chavanne et al., "Prospects for the use of permanent magnets in future accelerator facilities", in Proc. IPAC2014, Dresden, Germany, doi:10.18429/JACoW-IPAC2014-TUZB01.
[7] O. Chubar, P. Elleaume, J. Chavanne, Radia developed at ESRF, version 4.1. https://www.esrf.fr/Accelerators/Groups/InsertionDevices/Software/Radia
[8] M.Gehlot et al, "Design of Permanent Magnet Dipoles-Quadrupoles with Longitudinal Gradient for the PETRA IV Storage Ring", in Proc. IPAC2023, Venice, Italy, doi/jacow-ipac2023-wepm100.